This Project has received funding from European Commission by means of Horizon 2020,
the EU Framework Programme for Research and Innovation, under Grant Agreement no.727348

Grant Agreement No. 727348

Project Acronym:

SOCRATCES

Project title:

SOlar Calcium-looping integRAtion for Thermo-Chemical Energy Storage.

DELIVERABLE D2.3

Optimum heat integration carbonator-power cycle for SOCRATCES project

Funding scheme:	Research and Innovation Action (RIA)		
Project Coordinator:	USE		
Start date of the project:	01.01.2018	**Duration of the project:**	36 months
Contractual delivery date:	Month 12		
Actual delivery date:	28.12.2018		
Contributing WP:	WP2		
Dissemination level:	*Public*		
Authors:	Pau Giménez, Carlos Ortiz (USE)		
Contributors:	Ricardo Chacartegui (USE)		
Corresponding author	Carlos Ortiz (University of Seville-USE): cortiz7@us.es		
Version:	V1		
Document name	**SOCRATCES_D2.3_final**		

Table of contents:

LIST OF TABLES

LIST OF FIGURES

INTRODUCTION

This document analyses the heat transfer mechanisms associated to the carbonator reactor looking for optimizing the carbonator-power cycle heat integration. The aim of this document is to provide relevant information to be considered within the WP2 and WP6, facing the carbonator design and construction.

A carbonator heat transfer model has been developed to evaluate the carbonator behaviour under relevant operation conditions for the SOCRATCES project. The model considers the carbonation kinetics within a 1-D reactor model. This work, which is mainly focused on heat transfer mechanisms and their effect on carbonator design, is fully complementary to the carbonator models proposed within the task 2.2 (Deliverable 2.2), in which complex fluid dynamics mechanisms were included. Thus, all the carbonator models proposed within the WP2, each one developed and oriented from a specific perspective compose a complete framework about the reaction behaviour and the implications facing the prototype construction (i.e. in this deliverable with focus on evaluation of the heat transfer mechanisms and their effect over carbonator design).

The scope of the model described in this document is to provide a useful tool to evaluate the heat transfer from the highly-exothermic carbonation, providing in this way worthy information for the carbonator design (WP2) as well as for the prototype design within the EPC task (WP6). Therefore, at this stage, this document should not be understood as a closed work, but as a **framework that allows the development of different analyses to be developed in the next months (see subtask ST2.3. below) as support for the carbonator design and looking for the optimum conditions to carry out the energy release in the reactor.** The model developed within this deliverable allows evaluating the effect of different design and operation parameters on heat delivery in the carbonator. Carbonator size, operating conditions (P, T) or even changes in CaO precursors can be analysed from this model.

This deliverable summarizes the work under execution in *Task 2.3 "Heat integration"*. This task is divided into the following activities or subtasks:

- ST 2.3.1: Thermodynamic characterization of the carbonator and energy released in the carbonation reaction.
- ST 2.3.2: Interaction with WP4/task 4.1 (Carbonation power cycle integration).
- ST 2.3.3: Write-up of reports (D.2.3. Carbonator Energy Analysis)
- ST 2.3.4: Interaction with other technical WPs and tasks.

The deliverable has the following structure: the first section describes the carbonator reactor under development within the SOCRATCES project and the main heat transfers mechanism associated to the heat release from the exothermic carbonation reaction. Later on, the proposed heat transfer model is described in detail, from the main assumptions to the full model formulation. Finally, as examples of the potential of the model to support the carbonator design activity, the model is used to generate results under representative conditions. They are shown in section 3.

The document here presented has been developed by University of Seville within the SOCRATCES project under the confidentiality rules of the project and consortium.

1. CARBONATOR HEAT TRANSFER MECHANISMS

A proper understanding of the heat transfer mechanisms is needed to properly analyze the heat released in the carbonator reactor and its capacity for power generation. Among the possible configurations for the carbonator-power cycle integration, which was analyzed in detail in the *Deliverable D4.1 "Carbonator energy analysis",* the present document is mainly focused on an indirect integration between both systems which is the selected configuration for the SOCRATCES prototype.

The carbonator configuration (downer reactor, Fluidized bed, etc.) geometry and operation conditions (pressure, temperature, gas and solids velocities, etc.) highly conditions the heat transfer from the reactor bulk to the heat transfer fluid (HTF) and therefore the power production, which shows the importance of properly evaluating the heat transfer mechanisms in the reactor.

An entrained flow reactor (downer) is proposed as carbonator within the SOCRATCES prototype. This configuration allows using fine particles and could facilitate the particles-gas separation in the closed loop. In the conceptual design, the reactor will be able to handle particles with average size around 60 µm. Figure 1-1 shows the preliminary design scheme of the carbonator reactor and the integration with the Stirling engine, as proposed by CERTH.

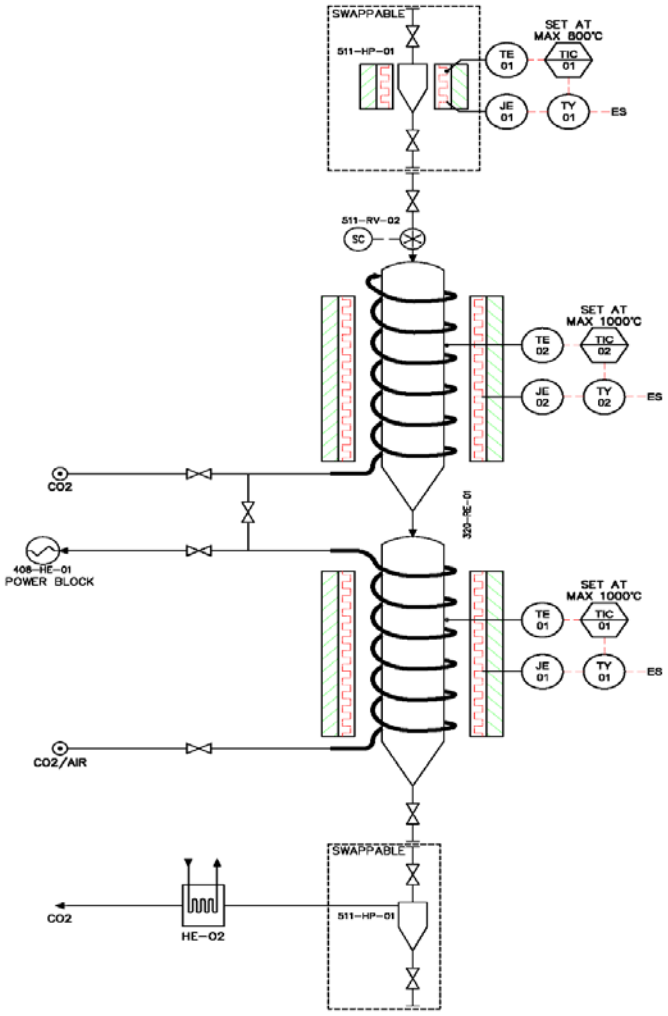

Figure 1-1. Conceptual carbonator scheme for the SOCRATCES prototype. Preliminary design scheme of the carbonator reactor (figure developed by CERTH). Taken from Deliverable 4.1

The reactor, which is divided in two sections, is kept at constant temperature by means of electrically heated furnaces. Hot CaO (previously preheated by an electric furnace in the solids vessel) is introduced from the top of the reactor as a free flow. The CO_2 is also introduced hot from the top of the reactor to follow a co-current flow with particles, being previously preheated by the carbonation heat/electric furnaces. The solids exit the reactor at the bottom and they are collected in the vessel downwards of the reactor. The CO_2 entering the carbonator is preheated from a spiral heat exchanger along the wall of the first section of the reactor. Heat of reaction will be exploited by an HTF (CO_2) running inside another spiral allocated in the second section of the reactor. The length of each section is predetermined at 2 m while the diameter has been set to 0.16 m.

The carbonator will be operated at isothermal conditions, keeping constant the temperature by using electric heaters in order to make independent and fully controllable the carbonation processes and to assure stable operating conditions. The heat transfer rate in the downer reactor is closely related to the hydrodynamics, with solids suspension density being the most influential factor [1]. The higher solids holdup the higher heat transfer coefficient. This issue is important for SOCRATCES carbonator since it works at very low solids handling.

The heating up process of the HTF through the spiral (heat coming from both electrical furnaces and carbonation inside the reactor) is simulated assuming annulus flow in 2 concentric pipes and matching the residence time and the heat transfer of the spiral pipe by adjusting the external dimeter (see section 2.1). The correlation of Kays and Perkins [2] for laminar through circular ducts is used to calculate the convective heat transfer while the CO_2 inside the spiral is considered transparent for the radiation calculations between external and internal wall of the annulus space. Conduction heat is calculated assuming steel pipe (k=15W/(m·K)) with a thickness of 5 mm.

Following with the analysis, among the different convection correlations between the wall and the cloud the one proposed in Spinelli et al. [3] is used:

$$Nu_{gw} = (0.023\, Re^{0.8}\mathrm{Pr}^{0.3})\left(1 + 4\, Re^{-0.32}\frac{\dot{m}_s}{\dot{m}_g}\frac{C_{p,s}}{C_{p,g}}\right)$$

Regarding radiation from wall-to-particles (or vice versa), as proposed in the WP3, a model for calculating absorptivity and emissivity of the gas-particle cloud is applied [4]. Finally, convection between gas and particles is neglected because of assuming the same velocity in both. Table 1 summarizes the heat transfer mechanisms analyzed in the carbonator.

Table 1: Summary of heat transfer mechanisms in the carbonator

Id.	Heat transfer mechanism	Description	Correlation
Q^{CV}_{we} Q^{CV}_{wei}	Convection external and internal wall of the annulus space to CO_2	Simulate the spiral flow; annulus flow in 2 concentric pipes is used to match the residence time of the spiral pipe (adjusting external diameter).	Correlations used for the simulated geometry D_h **Kays and Perkins** for laminar flow although it will be adjusted for the spiral convective heat transfer.
Q^{RD}_{we} Q^{RD}_{wei}	Radiation between external and internal wall of the annulus space	CO_2 is considered transparent to the radiation (this might not be true at high temperature). However the calculated emissivity of CO_2 is <0.1 $Q^{RD}_{we}=- Q^{RD}_{wei}$	View factor =1
Q^{CD}	Conduction through the reactor wall	Steel pipe k=15W/mK, thickness of 5 mm	
Q^{CV}_{wii}	Convection wall-GasParticles	According to Spinelli et al. [3] Nu=3.66	According to Spinelli et al. [3] (high v 1-4 m/s) According to Cengel [5] Nu=3.66 (constant Tw) Laminar Flow
Q^{RD}_{wii}	Radiation wall-GasParticles	**Model 1:** only convection (CO_2-particles) transparent to radiation. Generated heat removed trough convection. **Model 2:** opaque CO_2-CaO flow. View factor wall-fluid=1. Heat radiation between 2 concentric cylinders with the same radius. **Model 1 and 2** are the limiting cases for the real heat transfer process in the carbonator.	According to Siegel [6]: Leckner's correlations for the emissivity of CO_2=f(p·L,T) Differences between
	Convection Gas-Particles	Neglected. Same speed.	

2. CARBONATOR HEAT TRANSFER MODEL

2.1. Assumptions

In order to model the heat transfer mechanisms involved inside the carbonator reactor the following assumptions have been made:

- The gas-particle domain is an entrained downer-flow moving both species at the same speed.
- The gas removed in the carbonator as consequence of the reaction is not considered for the fluid dynamics for this first model.
- There is not convection between the particle and gas (no relative movement between them are considered)
- Uniform temperature is considered for the solid throughout the particle.

- Heat transfer (radiation and convection) is produced in the radial direction between the particle-gas and the wall tube
- A one dimensional model is considered with a constant and uniform temperature, particle concentration and distribution in each control volume.
- Convection and radiation occur between the gas-particle and the wall for each axial discrete volume.

This model evaluates the heat integration (Task 2.3) taking data from the carbonator kinetics results (Task 2.1) and carbonator model (Task 2.2) in order to evaluate the amount of energy that can be provided to the Stirling power cycle. Table 2 summarizes the initial data taken for modeling the SOCRATCES prototype carbonator.

Table 2. Initial consideration for the SOCRATCES prototype operation (from Deliverable D4.1)

CARBONATOR	
Type of reactor	Entrained flow reactor
Design temperature	800ºC
Design pressure	1 bar
Design thermal power	10 kWt
Design CaO flow rate	5-180 kg/h
Design CO_2 flow rate	7-16 kg/h
Preliminary reactor length	4 m
Preliminary reactor diameter	0.16 m
Median particle size, Dv (50)	60µm
Heat exchanger	External Spiral
Auxiliaries	Electric heaters (10-12 kWe)
POWER CYCLE	
Thermal power plant	Stirling engine
Design maximum thermal power	10 kWt
Working fluid	CO_2

2.2. Heat transfer model

The heat transfer model considers an annulus flow in contact with a constant wall temperature to preheat the CO_2 stream before entering the carbonator reactor. The CO_2 stream is considered transparent to radiation and absorbs heat through convection form both walls that forms the annulus space. The residence time of the CO_2 stream is adjusted to match the conditions of the spiral flow. Other modifications can be introduced in order to match the convective heat transfer coefficient in the spiral flow instead of the residence time. Heat transfer through radiation is exchanged between the two walls forming the annulus space.

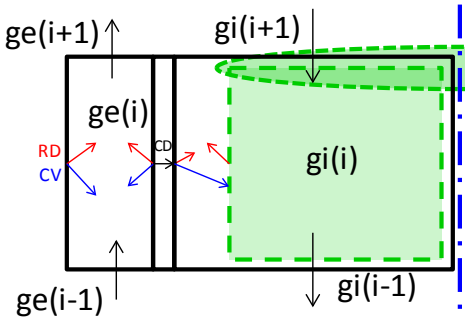

Figure 2-1. Heat transfer mechanisms considered in the model. Radiation (red), convection (Blue), conduction (black). External CO_2 stream (ge) and internal CO_2+particle stream (gi)

The energy balance is applied to the control volume (ge), the control volume (gi), the external surface of the reactor wall and internal surface of the reactor wall. The external wall temperature is maintained at a constant temperature, which is calculated by the model in order to achieve the desired temperature at the annulus space outlet which coincides with the reactor inlet (at the top). For j=1 to n_{wall} (number of sections of the reactor tube) the energy balance at the annulus space can be written as:

$$\dot{m}\cdot\left[h_{ge,2\cdot j-1}+\frac{v_{ge,2\cdot j-1}{}^2}{2}+g\cdot z_{2\cdot j-1}\right]+\dot{Q}^{CV}_{we,j}+\dot{Q}^{CV}_{wei,j}=\dot{m}\cdot\left[h_{ge,2\cdot j+1}+\frac{v_{ge,2\cdot j+1}{}^2}{2}+g\cdot z_{2\cdot j+1}\right] \quad \textit{Eq. 2-1}$$

Where the different heat flows in the equation are quantified by:

$$\dot{Q}^{CV}_{we,j}=h^{CV}_{we,j}\cdot A_{we}\cdot\left(T_{we,j}-T_{ge,2\cdot j}\right) \quad \textit{Eq. 2-2}$$

$$\dot{Q}^{CV}_{wei,j}=h^{CV}_{wei,j}\cdot A_{wei}\cdot\left(T_{wei,j}-T_{ge,2\cdot j}\right) \quad \textit{Eq. 2-3}$$

$$T_{ge,2\cdot j}=\frac{T_{ge,2\cdot j-1}+T_{ge,2\cdot j+1}}{2} \quad \textit{Eq. 2-4}$$

$$\dot{Q}^{RD}_{we,j}=K_{wewei}\cdot\sigma\cdot\left[T_{we,j}{}^4-T_{wei,j}{}^4\right] \quad \textit{Eq. 2-5}$$

Where K_{wewei} is the radiant constant between two concentric cylinders with emissivities ε_g for the internal cylinder and ε_w for the internal wall of the carbonator tube with the same diameter.

$$\dot{Q}^{RD}_{wei,j}=-\dot{Q}^{RD}_{we,j} \quad \textit{Eq. 2-6}$$

The required power to maintain the wall temperature constant is calculated by:

$$Pot_{w,j}=\dot{Q}^{RD}_{we,j}+\dot{Q}^{CV}_{we,j} \quad \textit{Eq. 2-7}$$

The energy balance at the external and internal wall surface are:

$$\dot{Q}^{CD}_{j}=\dot{Q}^{CV}_{wii,j}+\dot{Q}^{RD}_{wii,j} \quad \textit{Eq. 2-8}$$

$$\dot{Q}^{CD}_{j}+\dot{Q}^{CV}_{wei,j}+\dot{Q}^{RD}_{wei,j}=0 \quad \textit{Eq. 2-9}$$

$$\dot{Q}^{CD}_{j}=\frac{T_{wei,j}-T_{wii,j}}{R^{CD}};\ R^{CD}=\frac{ln\left(\frac{D_e}{D_i}\right)}{2\pi kL} \quad \textit{Eq. 2-10}$$

Where R^{CD} is the thermal conduction resistance of a steel cylinder.

The energy balance at the reactor control volume can be written as:

$$\dot{m}\cdot h_{gi,2\cdot j+1}+(\dot{m}+\dot{m}_s)\cdot\left[+\frac{v_{gi,2\cdot j+1}{}^2}{2}+g\cdot z_{2\cdot j+1}\right]+\dot{m}_s\cdot Cp_{s,2\cdot j}\cdot T_{gi,2\cdot j+1}+\dot{Q}^{CV}_{wii,j}+\dot{Q}^{CR}_{wii,j}+\dot{Q}^{GN}_{c,j}=$$
$$\dot{m}\cdot h_{gi,2\cdot j-1}+(\dot{m}+\dot{m}_s)\cdot\left[\frac{v_{gi,2\cdot j-1}{}^2}{2}+g\cdot z_{2\cdot j-1}\right]+\dot{m}_s\cdot Cp_{s,2\cdot j}\cdot T_{gi,2\cdot j-1}\qquad \textit{Eq. 2-11}$$

which considers the enthalpy of the CaO particles and CO_2 flow.

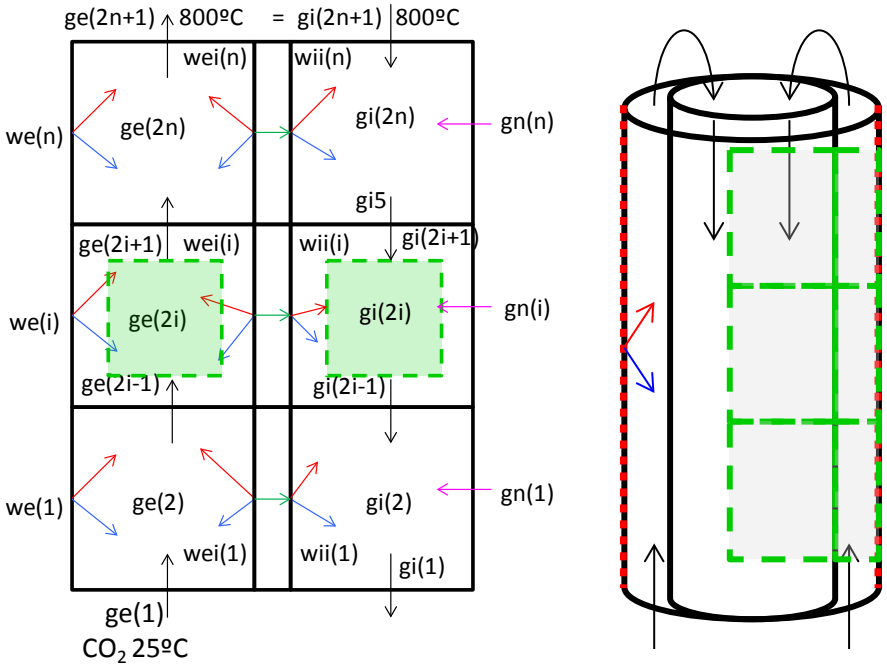

Figure 2-2. Model design: gn: reaction enthalpy released; w: wall; i: interior; e: exterior; g: gas

2.3. Radiation Modelling

Four different approaches have been considered in order to quantify the thermal radiation exchanged between the particle-gas cloud and the reactor wall, from the lower to the higher complexity. Radiation between wall and gas/particles.

- Approach-0: only convection model (particles gas stream transparent to radiation). No radiation is considered because there is only one surface (internal reactor surface).
- Approach-1: radiation between two concentric cylinders with the same radius (particles gas stream opaque to radiation). For this approach the emissivity of the gas (ε_g) can be modified between [0.1 –1] which would simulate the two most extreme cases.
- Approach-2: radiation between a participating medium (CO_2) and the internal wall surface. The CO_2 emission and absorption coefficients must be determined (ε_g and α_g).
- Approach-3: radiation between the particle cloud stream and the internal wall surface. The absorption and backscatter radiation have to be introduced depending on the particle size and concentration. CO_2 is considered transparent to radiation.
- Approach-4: radiation between a participating medium (CO_2+particles) and the internal wall surface. The CO_2+particle emission and absorption coefficients must be determined (ε_{g+p} and α_{g+p}).

For the different approaches the radiation is transferred only in the radial direction, which means that there is no radiation exchanged between the wall of the reactor of one section and the adjacent sections neither between the cloud of one section and the adjacent volumes. This assumption would be more accurate when the number of sections is low and less accurate when

the number of sections is high as follows: each control volume is a cylinder of dimensions D and ΔL (12.9 cm). When the aspect ratio (ΔL/D) of the cylinder increases, increasing the number of sections in which the reactor length has been divided, the control volume resembles more a disk than a cylinder, and the cross-sectional area of the control volume becomes more important than the reactor wall area. In this case a new approach-5 has to be considered with a new heat radiation exchange between the adjacent control volumes of the CO_2-particle cloud.

The radiation heat transfer following the approach-1 can be written as follows, where the main assumptions are that the gas-particle stream are opaque to radiation and ε_g is the emissivity of the cloud. By changing the emissivity, we can evaluate the extreme cases and to have an estimation of the most extreme solutions to the problem, as framework for carbonator design.

$$\dot{Q}_{gw} = \frac{A \cdot \sigma \cdot (T_g^4 - T_w^4)}{\frac{1}{\epsilon_w} + \frac{1}{\epsilon_g} - 1} = K_{wewei}\sigma(T_g^4 - T_w^4)$$

The radiation heat transfer using the approach-2 model can be calculated as flows:

$$\dot{Q}_{gw} = A\sigma \frac{\epsilon_w}{1 - (1 - \epsilon_w)(1 - A_v)}(\epsilon_g T_g^4 - A_v T_w^4)$$

Where ε_g is the emissivity of the gas and A_v is the geometry-dependent absorptance. The value of ε_g varies with pressure, optical thickness and temperature. It is found using the Figure 2-3.

The absorptance A_v is a function of the wall and gas temperatures and the emissivity of the gas:

$$A_v = f_{p,CO_2}\left(\frac{T_g}{T_w}\right)^{0.65} \epsilon_g$$

The above development is valid for CO_2. Note that $f_{p,CO2}$ is a pressure correction factor with value 1 at a total pressure of 1 bar . For the absorptance the emissivity must be evaluated at the wall temperature, and with the mean beam length as $s_{eq} \cdot p_{CO2} \cdot \frac{T_w}{T_g}$. The mean beam length can be estimated with:

$$s_{eq} = 0.9 \cdot \left(\frac{4V}{A}\right)$$

The emissivity of a cloud of limestone in CO_2 (approach-4) is calculated based on the *SOCRATCES calciner working document v1.5*, which in turn is taken from VDI Heat Atlas, Part K [4]. The flux from the gas-particle mixture to the wall, $q_{g+p,w}$, is calculated by:

$$\dot{q}_{g+p,w} = \frac{\epsilon_w}{\alpha_{g+p} + \epsilon_w - \alpha_{g+p}\epsilon_w}\sigma(\epsilon_{g+p} T_g^4 - \alpha_{g+p} T_w^4)$$

The total emissivity of a gas-particle mixture can be described as:

$$\epsilon_{g+p} = (1 - \beta)\frac{1 - e^{-\Phi_{emi,g+p}}}{1 + \beta e^{-\Phi_{emi,g+p}}}$$

Where:

$$\beta = \frac{\gamma - 1}{\gamma + 1}; \qquad \gamma = \sqrt{1 + \frac{2\bar{Q}_{bsc}}{\bar{Q}_{abs}}}; \qquad \Phi_{emi,g+p} = \left(\bar{Q}_{abs} A\, L_p + K_{emi,g}\right) l_{mb}\gamma$$

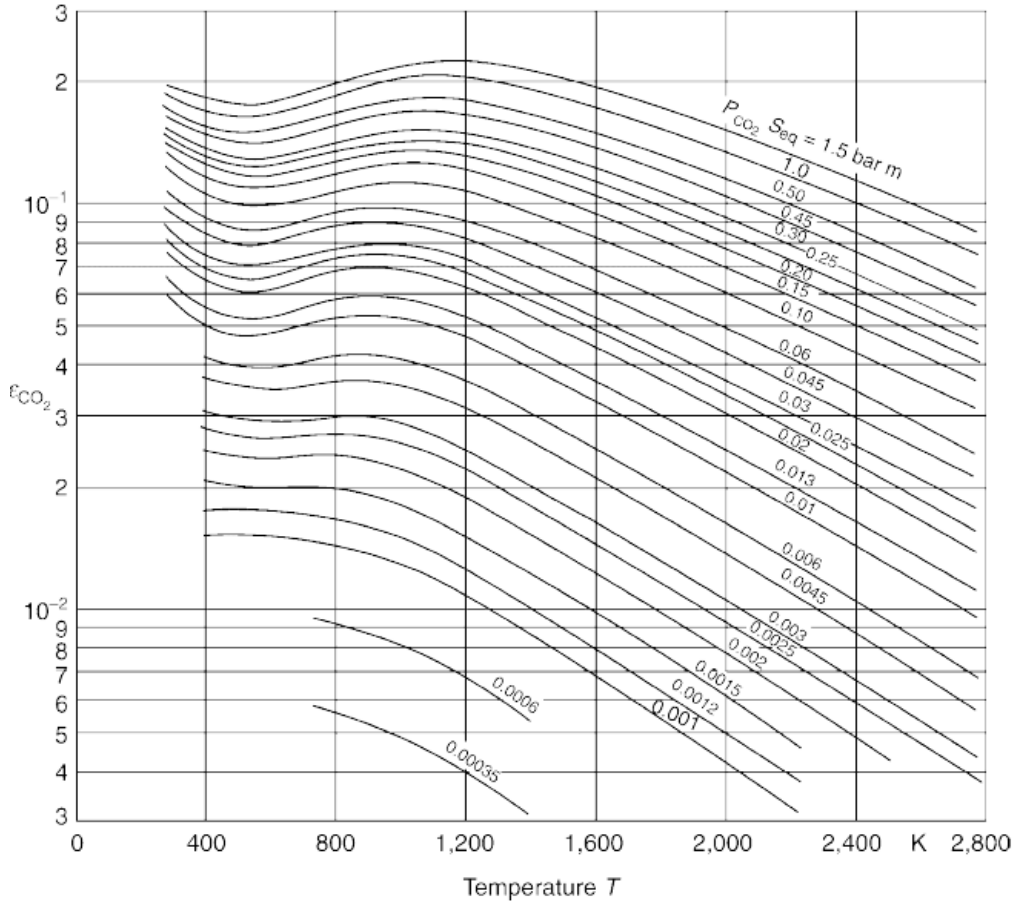

Figure 2-3: Emissivity of CO_2 at different optical thicknesses and temperatures, at 1 bar. Note that s_{eq}, , equivalent layer thickness, is identical to l_{mb} the mean beam length.

In a similar manner the absorptivity can be calculated:

$$\alpha_{g+p} = (1-\beta)\frac{1-e^{-\Phi_{abs,g+p}}}{1+\beta e^{-\Phi_{abs,g+p}}}$$

Where:

$$\Phi_{abs,g+p} = \left(\bar{Q}_{abs} A\, L_p + K_{abs,g}\right) l_{mb}\gamma$$

L_p is the particle loading, in kg/m^3. The parameter l_{mb} is the mean beam length of radiation within the relevant geometry.

A is the specific projected surface area of the particles, in m^2/kg. In order to determine the particle absorption and scattering coefficients Q_{abs} and Q_{bsc} the information from the graphical representation has been extracted and adjusted. VDI heat atlas [4] provides the values for limestone. The mean particle diameter d_p is measured experimentally, or can be calculated from the projected surface area and density of the particles by:

$$d_p = \frac{3}{2\rho_p A}$$

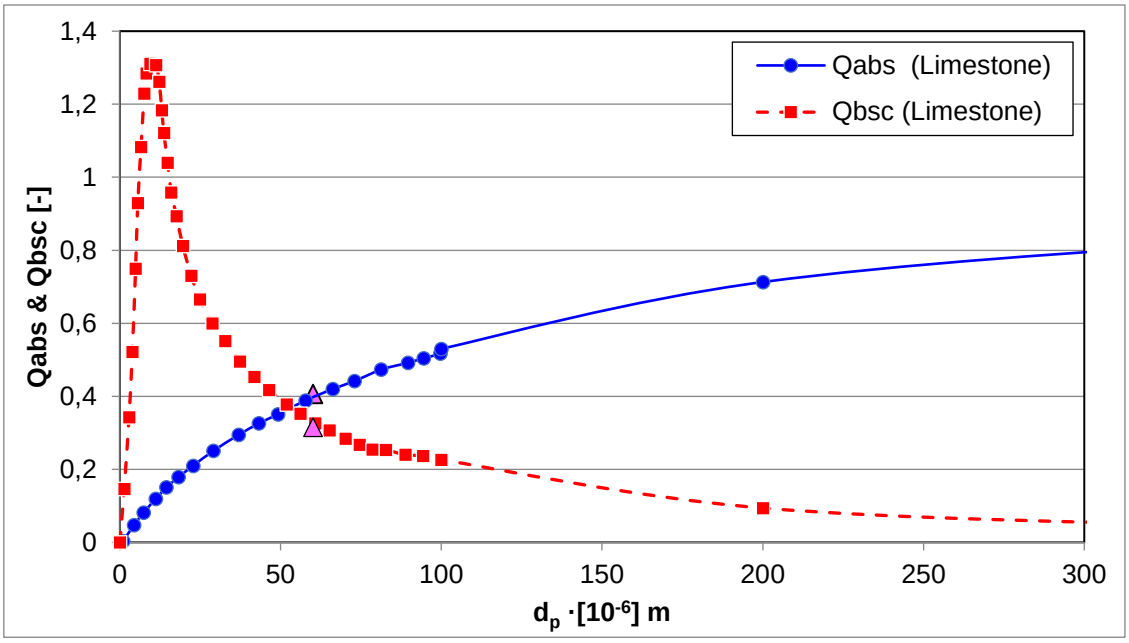

Figure 2-4: Absorption and Backscattering coefficients for limestone as a function of mean particle diameter. Purple triangles are the values for 60µm particle limestone. Extracted from VDI heat atlas [4]

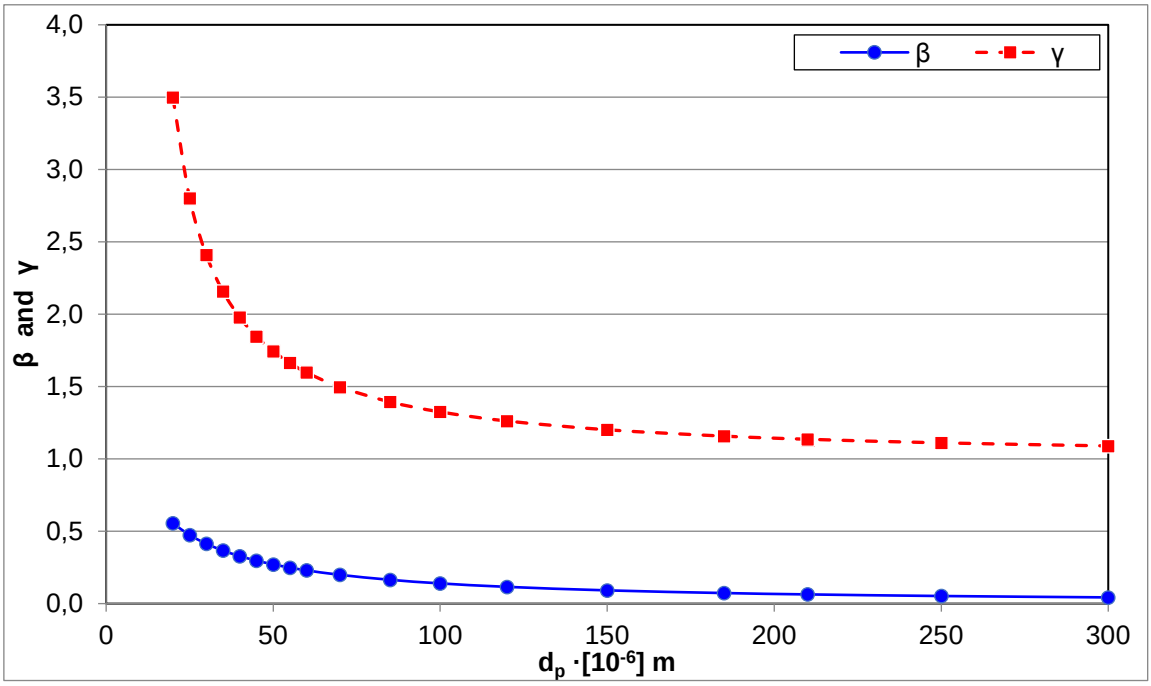

Figure 2-5: γ and β parameters as a function of mean particle diameter required to calculate the emissivity and absorptivity of the gas+particles (ε_{g+p} and α_{g+p}). Extracted from VDI heat atlas [4]

The absorption and scattering coefficients $K_{abs,g}$ and $K_{emi,g}$ can be determined as:

$$K_{emi,g} = -\frac{\ln(1-\epsilon_g)}{l_{mb}}; \qquad K_{abs,g} = -\frac{\ln(1-A_v)}{l_{mb}}$$

From the previous correlations, the approach 4 has been implemented in the model for calculating the radiation inside the carbonator.

2.4. Modelling convection

The model considers the convection between the external annulus space and the CO_2 stream, and the convection between the reactor wall and the CO_2+particles stream. Different correlations have been evaluated to simulate these two heat transfer mechanisms. The external annulus space represents the spiral tube in the heat transfer model. The external diameter is adjusted to match the residence time of the fluid in the spiral flow. In order to estimate the spiral convection coefficient the following correlations have been used based on Incropera and DeWitt [7] for a completely developed flow in a pipe straight pipe (as a first approach).

$Re = \frac{v \cdot D}{\nu}$; $Nu = \frac{h \cdot D}{k}$; $f = (0.79 \cdot \ln(Re) - 1.64)^{-2}$; (Petukhov correlation for f) [7]

$Nu = \frac{(f/8)(Re-1000)Pr}{1+12.7(f/8)^{1/2}(Pr^{2/3}-1)}$; (Gnielinski correlation for $3e^3 < Re < 5e^6$) [7]

Table 8.1 in [7] reports the Nusselt numbers for fully developed laminar flow in tubes. The contribution of the particles regarding convection is not considered at this point. For the annulus the hydraulic diameter is calculated as the characteristic length for the external and internal Nusselt number correlation. For a laminar flow the internal and external Nusselt number have been obtained based on Table 8.2 [7] for a circular tube annulus with one surface insulated and the other at constant temperature. Even though this correlation is only appropriate for the section of the carbonator that transfers heat to the Stirling heat transfer fluid, it has been used for the complete annulus space. An updated version of this model will include the Table 8.3 correlation: "Influence coefficients for fully developed laminar flow in a circular tube annulus with uniform heat flux maintained at both surfaces" [7].

Although the spiral flow is expected to show a higher heat transfer correlation than the one calculated in the heat transfer model, the larger heat transfer area of the modelled system is expected to compensate partially this effect. Another approach would be to calculate the convection coefficient based on the annulus flow and to adjust the external diameter to match the heat transfer in the spiral flow. In this case the residence time would be lower than the spiral one. For the reactor convection coefficient different correlations have been evaluated. The first one based on the "*Deliverable 2.2: carbonator model (UNIZAR)* ".

$$Nu = 3.66 + \frac{\left[0.049 + \frac{0.02}{Pr}\right] Gz^{1.12}}{1 + 0.065 \cdot Gz^{0.7}}; Gz = \frac{Re \cdot Pr}{\left(\frac{L}{D}\right)}$$

The second correlation evaluated is based on Spinelli et al. (2018) [3]:

$$Nu = 0.023 \cdot Re^{0.8} \cdot Pr^{0.3} \cdot \left[1 + 4 \cdot Re^{-0.32} \cdot \frac{\dot{m}_s}{\dot{m}} \cdot \frac{Cp_s}{Cp}\right]$$

where the sub-index "s" refers to the limestone particle stream (mass flow, and specific heat) instead of the CO_2 flow.

The convective coefficients obtained by these two correlations are similar in the range of

i) 1 - 2.2 W/(m^{2}K) for $\dot{m}_{CO_2} = 5\ kg/h$;

ii) 1.5 - 2.6 W/(m^{2}K) for $\dot{m}_{CO_2} = 10\ kg/h$

iii) 5 W/(m^{2}K) for $\dot{m}_{CO_2} = 50\ kg/h$

2.5. Carbonation kinetics

The carbonation kinetics introduced in the model is based on a Prout-Tompkins mechanism. Prout–Tompkins model function $f(X) = X(1-X)$ [8] is modified by introducing a conversion limit X_K (see Eq- 2-13 below), which is the CaO conversion at the end of the reaction controlled phase, as proposed in a previous work [9]. The temperature dependence of the reaction rate and consequently the extent of the reaction are considered.

$$\boldsymbol{r \approx a_2\, e^{-\frac{E_2}{RT}}\left(\frac{P}{P_{eq}}-1\right)\left(\frac{1}{\frac{P}{P_{eq}}+e^{\frac{\Delta S_2^0}{R}}\, e^{-\frac{\Delta H_2^0}{RT}}}\right)} \qquad \textit{Eq. 2-12}$$

$$\boldsymbol{\frac{dX}{dt} = X\left(1-\frac{X}{X_k}\right) r(T,P) \quad \leftrightarrow \quad X(t) = \frac{X_k}{1+e^{-r(t-t_o)}}} \qquad \textit{Eq. 2-13}$$

Table 3: CO_2 partial pressure at equilibrium and values of enthalpy-entropy changes in the chemical decomposition and desorption stage, and activation energies. Extracted from Ortiz el al. [9]**.**

$P_{eq}(\text{atm}) = 4.083x10^7\, e^{-\frac{-20474}{T}}$ [10]	
ΔH_r^0	180 kJ/mol
ΔH_1^0	160 kJ/mol
ΔH_d^0	20 kJ/mol
E_d	20 kJ/mol
E_1	180 kJ/mol
E_2	20 kJ/mol
ΔS_r^0	0.16 kJ/(mol·K)
ΔS_1^0	0.068 kJ/(mol·K)
ΔS_d^0	0.092 kJ/(mol·K)

The preexponential factor $\boldsymbol{a_2}$ has been inferred from experimental test carried out within the task 2.1 (carbonation kinetics). As first approximation for the analysis it has been taken a_2=11600 (1/s) (from OMYACARB 10 BE 100% at 800ºC results, see *Deliverable 2.2: carbonator kinetics*). Later on, in simulation 3, the effects of a faster kinetics have been analysed from a value of a_2=42255(1/s), which has been taken from AUTH results within the *Deliverable 2.2.*

Other CaO precursor as well as other operating conditions will be analysed through the model proposed in this document within the WP2. The conversion at the end of the kinetically-controlled stage mainly depends on the number of cycles and the temperature [9]. From TGA test carried out within the task 2.1, a tentative value of X_k=0.16-0.2 is considered for the simulations.

2.6. Flow in helical pipe

The first approach considers the helical pipe as annulus flow to preheat the CO_2 up to the carbonator temperature. The external annulus diameter is adjusted to achieve the same residence time of the CO_2 in the helical pipe as in the annulus flow. The helical flow will achieve a higher heat transfer convection coefficient. However, the main difference is the heat transfer area: while the helical pipe has a low heat transfer area, the annulus space has a higher area to transfer heat to the CO_2 stream. Due to the low heat transfer area of the helical pipe the temperature of the wall required to preheat the CO_2 stream is expected to be higher in the real system, although this effect is expected to be compensated by the higher convective heat transfer coefficient.

Correlations for a straight pipe are taken to estimate the convective heat transfer coefficient in the helical pipe when the CO_2 mass flows is preheated from 25ºC to 800ºC. The average velocity will be higher as well as the convective heat transfer coefficient. The calculated heat transfer coefficient is used as an input for the convective heat transfer coefficient in the annulus space. Correlations for this last flow pattern are also used in order to compare with the previous one.

2.7. Simulations

The model has been developed by using Engineering Equation Solver (EES). Table 4 shows a summary of methodology, inputs and outputs for the heat transfer carbonator model.

Table 4: Carbonator model summary

INPUTS
Inlet conditions of CO_2 and CaO (T, P) Carbonator design conditions (P, T) Carbonator dimensions Inlet conditions of the cooling and Stirling fluid Default particle size distribution has a volume-weighted median particle diameter of 60 μm
METHODOLOGY
Chemical reactions (Kinetics): Deliverable D2.1 Fluid-dynamics: plug flow for the gas Heat transfer: full model development by considering main heat transfer mechanisms. The model will be included within the Deliverable 2.3 Convection correlations: - Spinelli et al. [3]: flow inside the reactor - Concentric Pipes: flow in annulus space. Ref: [5]. Nusselt int y ext (laminar flow completely developed in an annular space with isothermal wall and adiabatic wall (Kays y Perkins) (simulating the spiral pipe) Gas-particles to wall: a) only convection (gas-particles transparent to radiation), b) only radiation c) Convection and radiation d) Axial radiation between control volumes i and i+1. CO_2 effective volumetric flow due to the presence of particles CO_2 mass flow variations due to adsorption
ASSUMPTIONS
Carbonator composed of 2 tubes of 2 meters long each Helical pipes around them for cooling. The cooling fluid (carbon dioxide) enters at the bottom in the first carbonator, while the Stirling fluid (carbon dioxide) enters at the top in the second carbonator. Constant pressure along the carbonator. Steady state conditions. Helical pipe flow modelled like an annulus counter current flow heat exchanger.
OUTPUTS
Reactor temperatures profile Reactor Power at length i and Total input power. Conversion and reaction rate at length i Wall temperature profile Flow conditions of the cooling and Stirling fluid at length i

3. MODEL SIMULATION RESULTS

This section shows the potential of the model to be used as tool to support the carbonator design, complimentary to the other specific models developed within SOCRATCES and that together define the complete design framework. On this purpose of showing the potential of the model, three complete simulations using the model are developed. These simulations are presented to show the performance and capabilities of the model but they are not applied to definitive design conditions. They will be defined in an iterative process within the next months under different conditions within the WP2 (subtask 2.3.4). The use of this model will to provide useful information facing the design and construction of the carbonator. It will include sensitivity analysis on different design and operating parameters: carbonator pressure and temperature, CaO precursors to be used, CO_2 mass flow entering the reactor or Stirling HTF fluids inlet conditions; about modeling issues, analyzing the particle diameter effect on the emission and absorption properties of the gas/particle cloud.

3.1. Simulation 1

Table 5. Parameter Simulation 1.

CARBONATOR			
Type of reactor	Entrained flow reactor	T_{in} CO_2 from storage [ºC]	25ºC
Design temperature	800ºC	T_{out} CO_2=T_{in} carb [ºC]	800ºC
Design pressure	1 bar	ε_{we}= ε_{wei}= ε_{wi}	0.8
Design thermal power	10 kWt	ε_g	0.12
Design CaO flow rate	5 kg/h	ε_{g+p} (calculated)	0.21
Design CO_2 flow rate	10 kg/h	ΔL	0.05 m
Reactor length	4 m (2 m+2 m)	h_{spiral} (calculated)	6-15 W/m^2K
Reactor diameter	0.16 m	Xk	0.2
Median particle size, Dv (50)	60µm	a_2	11600 s^{-1}

Figure 3-1 shows the temperature profile along the carbonator reactor and the annulus space. The CO_2 stream (red curve) enters at the bottom of the preheating section at 25ºC and it is heated up to achieve 800ºC at the outlet, just before entering the carbonator at the top. CaO particles enters the carbonator at 800ºC because of the previous preheating (see Figure 1-1). Note that CO_2 coming at 25º is the most conservative value, which will occur at the starting-up or if CO_2 comes directly for the storage. After the process starts, a certain amount of CO_2 exiting the carbonator at high temperature can be recirculated to the carbonator inlet once the solids are separated. This means that CO_2 will enter the preheating zone at much higher temperature.

Then the CO_2+particles are mixed and flow in the same stream along the downer reaction. As shown in the figure, the reactor is effectively cooled by the HTF preheating, taking the released for the highly-exothermic reactions and avoiding an excessive temperature increase that could stop the if equilibrium temperature is reached. Thus, Figure 3-2 shows how the reaction rate along the reactor is kept under adequate values without reaction stops. The materials exit the carbonator with a temperature around 780ºC, which is a proper temperature to continue the reaction in the second part of the reactor.

The residence time (7.2 s) depends on the CO_2 mass flow rate and the temperature which modifies the density. As pointed out in the assumptions, at this stage is considered that solids

and gas are moving at the same velocity through the downer. The extent of carbonation X as a function of reactor length can be observed in Figure 3-3. As may be seen, CaO particles leave the first 2m of reactor with a carbonation degree X= 0.063. Note that this analysis is carried out considering a previously cycled particles that, mainly because of the sintering, can reach a maximum conversion in the kinetic controlled stage of X_k=0.2. This means that CaO particles exits the first 2m of reactor with a 31.7% of the expected total conversion. As shown in Figure 3-4, this CaO conversion at the exit of the first carbonator section could be increase by increasing the residence time of the particles in the reactor. This is analysed in the second simulation of this section.

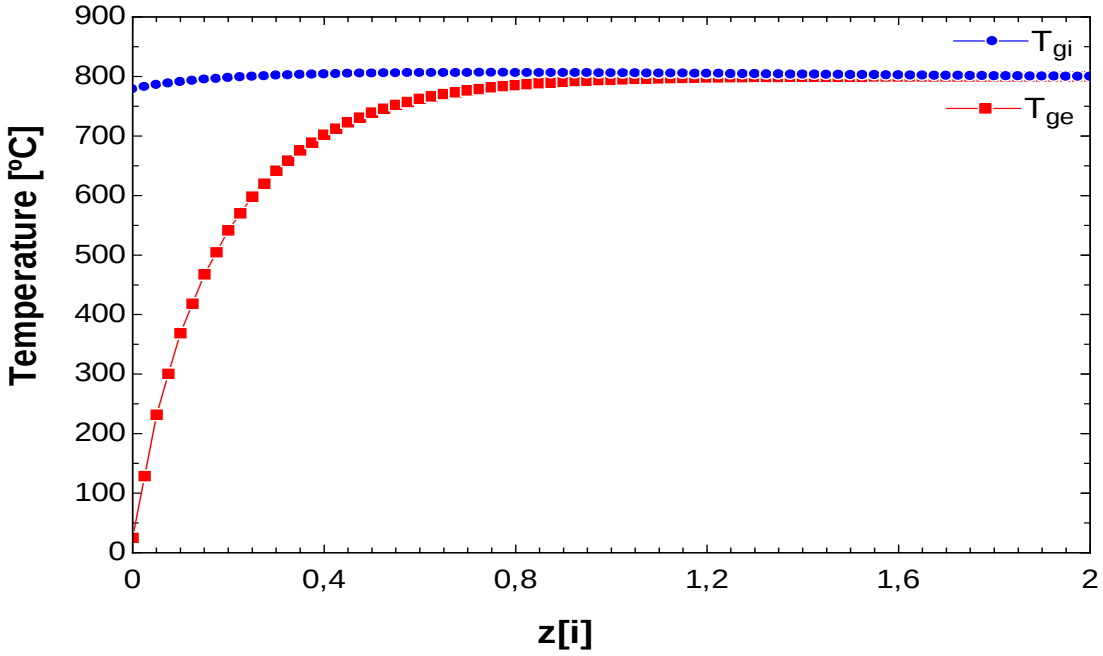

Figure 3-1. Temperature (ºC) profile vs reactor height (m).

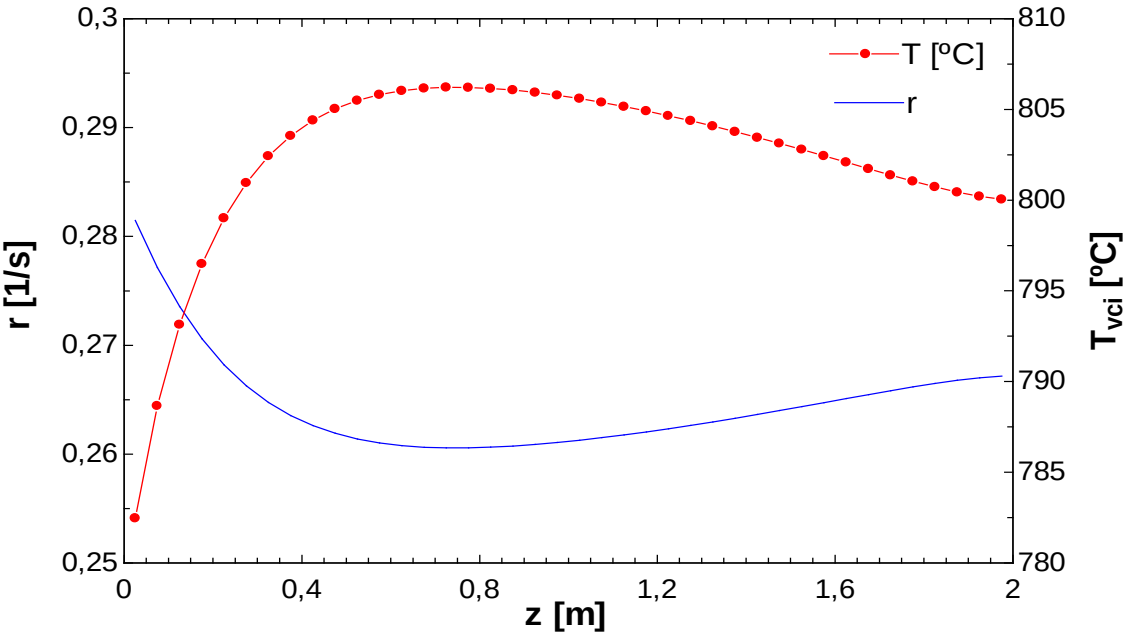

Figure 3-2: Reaction rate (1/s) and temperature (ºC) vs reactor height (m)

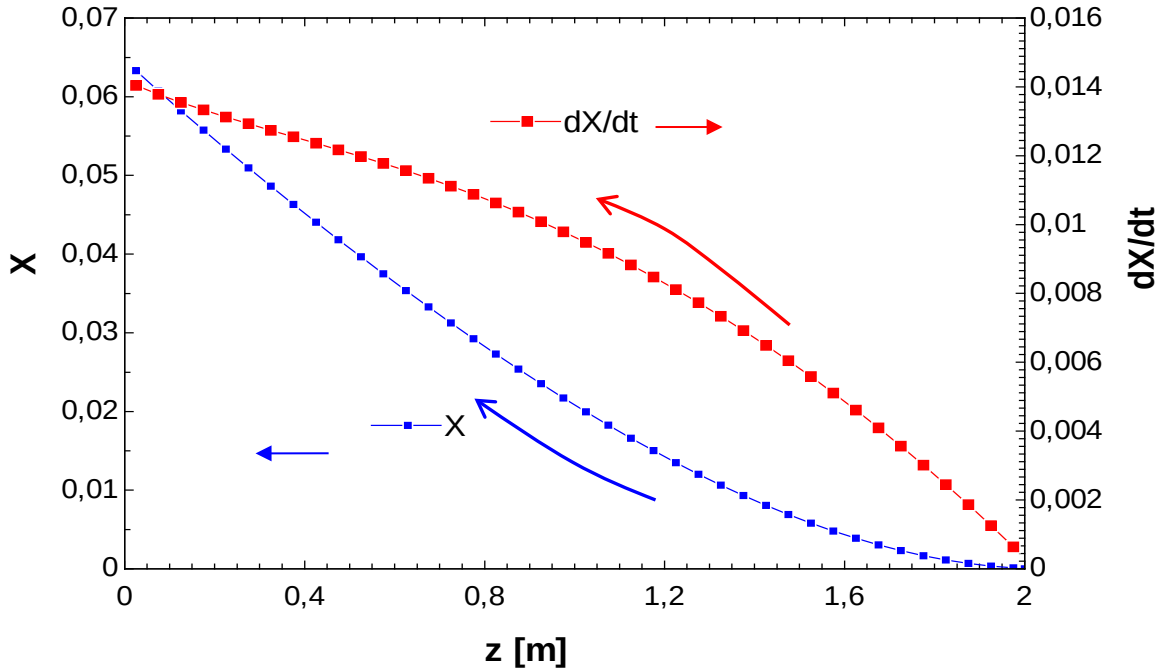

Figure 3-3: Extent of the reaction (blue) and its derivative vs the reactor height (m).

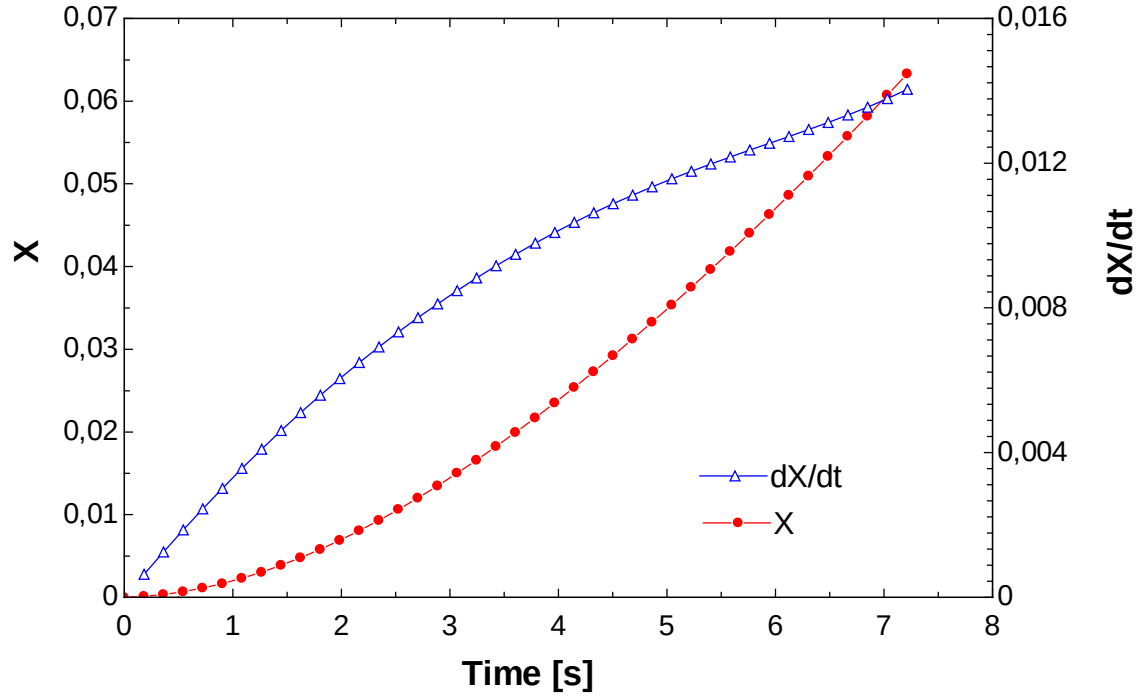

Figure 3-4. Extent of the reaction (red) and its derivative(blue) vs time

Figure 3-5 shows the external power requirements (from electric ovens or from any other source) to keep constant the reactor conditions along the whole time and departing from the above mentioned conditions. Note that this analysis considers reactor isothermal operation (T=800ºC). The required power to maintain the external wall temperature is large at the bottom of the reactor (the entrance of the annulus space where the CO_2 is entering at 25ºC). The required power lowers until z=1 m where it becomes slightly negative, which means that to

maintain the wall temperature constant cooling power is required. By integrating along the reactor, a total heating power 2 kW is required. However, the initial sections require 10kW/m.

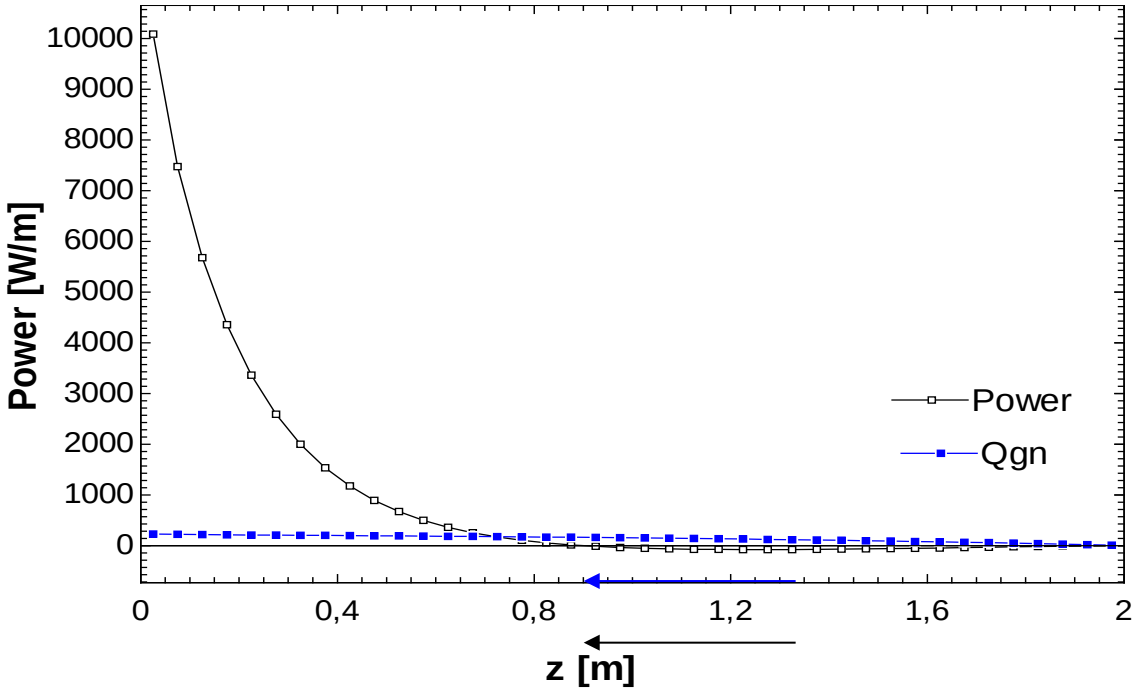

Figure 3-5. Power supplied (black) and power released by the carbonation reaction (blue) to maintain the external wall temperature at 800ºC.

Figure 3-6 shows the estimated heat transfer convection coefficients. The main difference between them is the consideration that the flow has not been completely developed. This consideration is taken into account in "Deliverable *2.2: carbonator model (UNIZAR)* ". However, it is worth to mention than the equivalent radiation coefficient is in the order of 50W/m^{2}K. It means that the three correlations are accurate enough to capture the heat transfer mechanisms.

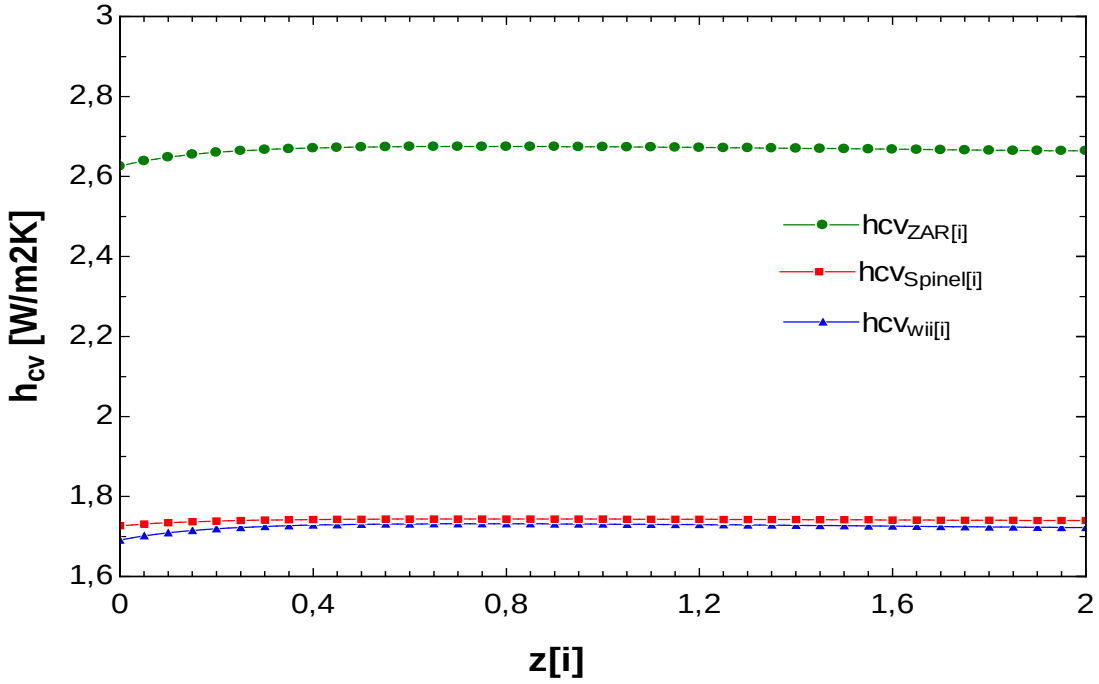

Figure 3-6. Heat transfer coefficients between the gas/particles stream and the carbonator reactor inner wall h (W/m2K) vs Z(m) using 3 different correlations: hcvSpine according to* [3]*, hcvzar according to SOCARTCES deliverable 2.2 and hcvw as calculated in the present model.

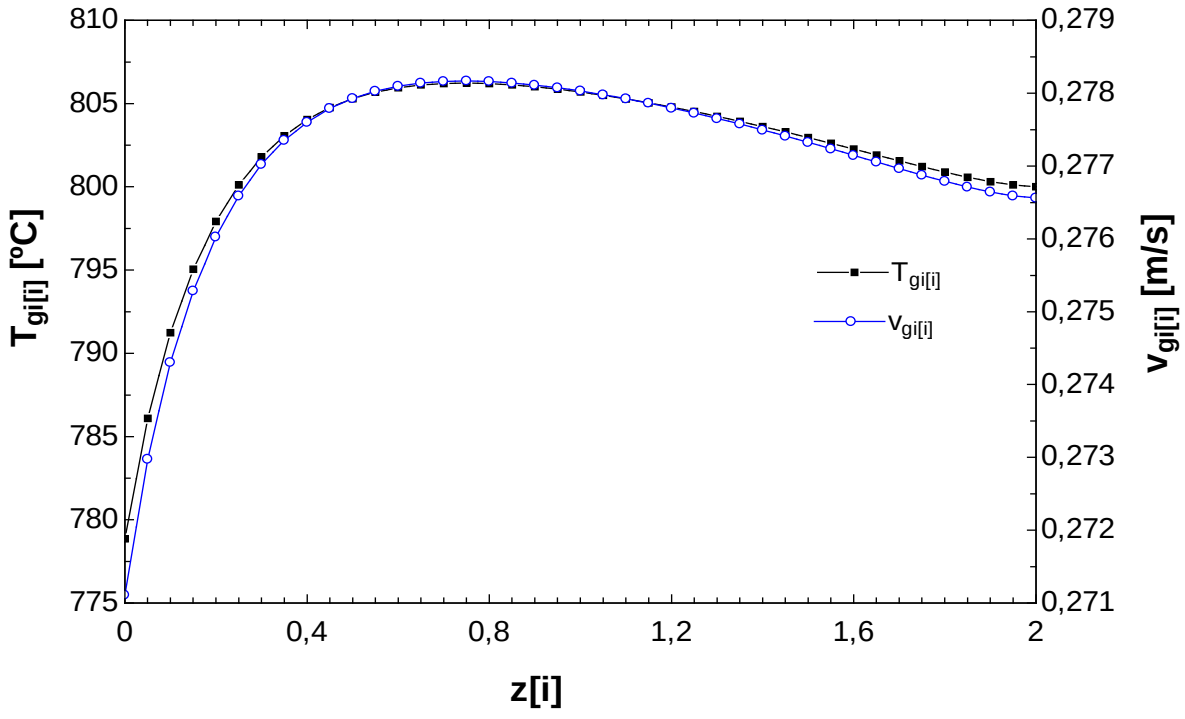

Figure 3-7. Temperature and velocity of the gas-particles stream vs reactor height (m)

The results obtained from the application of the model according to the simulation 1 are summarized in Table 6:

Table 6: carbonator results according to simulation 1

Extent of the reaction at the bottom of the carbonator reactor	0.06332
Fraction of the extent of the reaction	31.66%
Average Power supplied (min – max)	1000 W/m (-78 W/m to 10 kW/m)
Total power supply	2 kW
Temperature of the exterior wall	800ºC
Residence time	7.2 s

3.2. Simulation 2

In this new simulation the CO_2 mass flow has been halved. The different convection coefficients are reduced because of the lower velocity. The emissivity of the CO_2+particles stream increases because of the lower velocity. The external gas temperature reaches 800ºC at a lower height. This is shown in the table below, where main variations regarding the simulation 1 are highlighted in red.

Table 7. Parameter Simulation 2.

CARBONATOR			
Type of reactor	Entrained flow reactor	T_{in} CO_2 [ºC]	25ºC
Design temperature	800ºC	T_{out} CO_2=T_{in} carb [ºC]	800ºC
Design pressure	1 bar	ε_{we}= ε_{wei}= ε_{wi}	0.8
Design thermal power	10 kWt	εg	0.12
Design CaO flow rate	5 kg/h	ε_{g+p} (calculated)	0.29
Design CO_2 flow rate	5 kg/h	ΔL	0.05 m
Preliminary reactor length	4 m (2 m+2 m)	h_{spiral} (calculated)	3 - 6.5 W/m^{2}K
Preliminary reactor diameter	0.16 m	X_k	02
Median particle size, Dv (50)	60µm	a_2	11600 s^{-1}

Figure 3-8 shows the temperature profile along the carbonator reactor and the annulus space is represented. The behaviour is similar than in the previous simulation, but in this case the desired preheating value of the CO_2 coming for the storage is reach earlier, just in the first 0.4m of the reactor length.

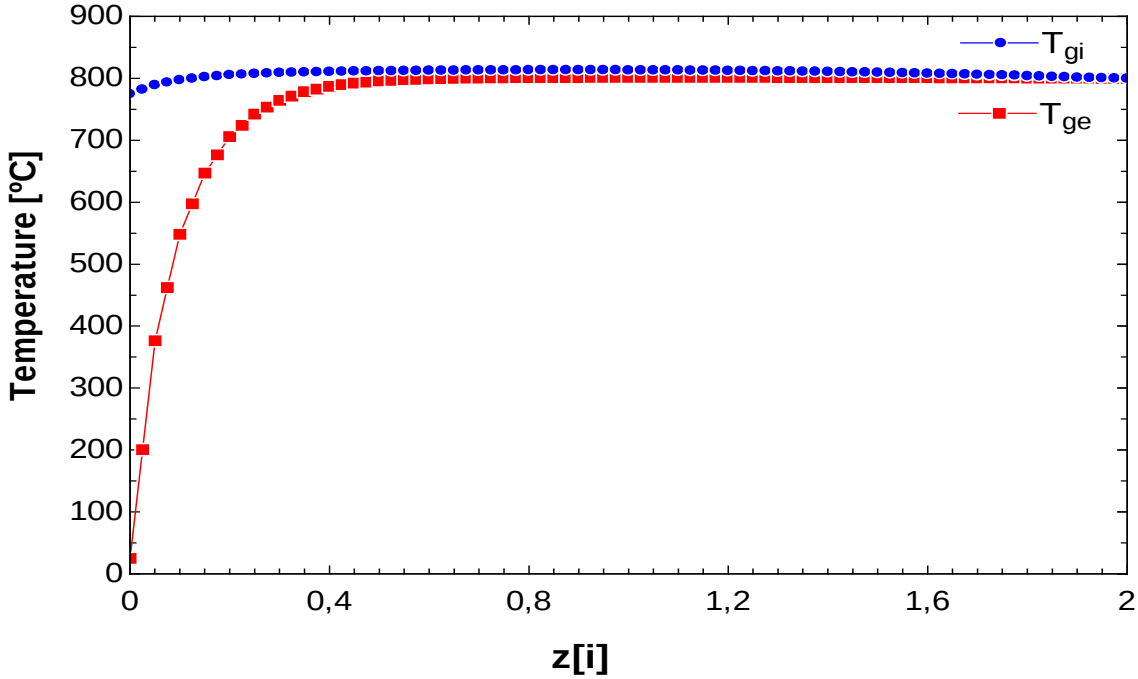

Figure 3-8. Temperature (ºC) profile vs reactor height (m) (simulation 2).

Because of the higher particles residence time under this conditions (14s instead 7s), CaO conversion reaches a value in the first carbonator section of X=0.137, which means a 68.6% of the expected maximum carbonation (see ***Figure 3-10*** and ***Figure 3-11***. It is important to remark that the higher conversion in the first carbonator section (preheat section), the lower maximum thermal power expected to be released for the Stirling in the carbonator section. Thus, a sensitive analysis will be required to optimize the power production varying, among other parameters, the mass flow rate of CO_2 entering the carbonator.

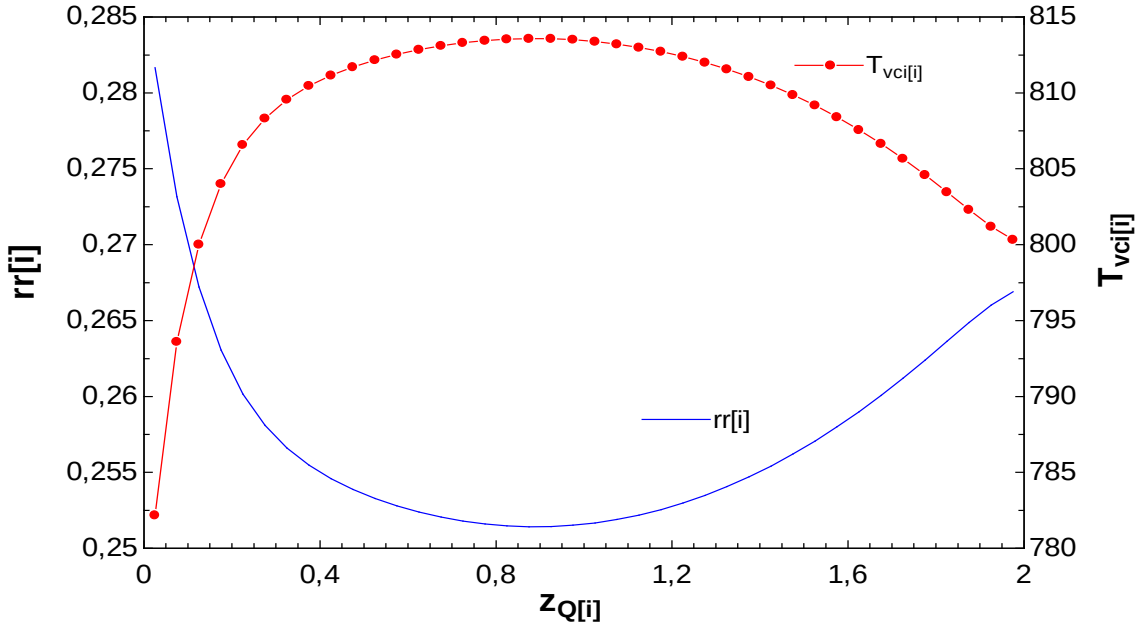

Figure 3-9: Reaction rate (1/s) and temperature vs reactor height (z in m) (simulation 2)

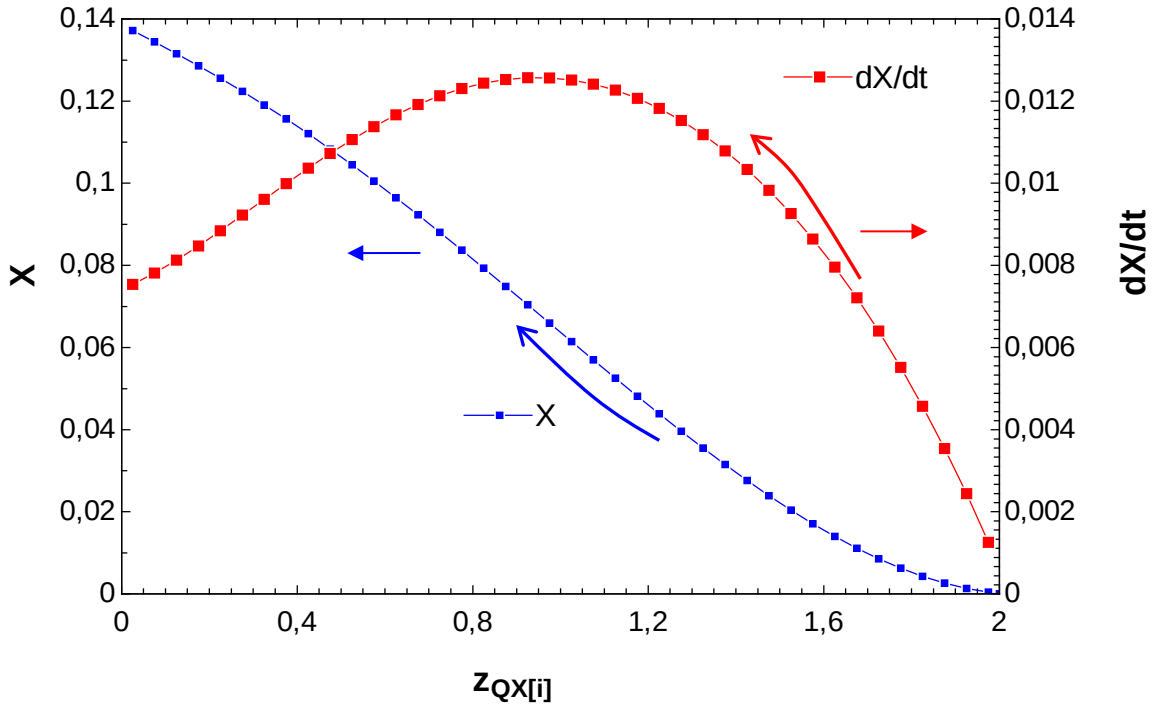

Figure 3-10: Extent of the reaction (blue) and its derivative vs the reactor height (m) (simulation 2)

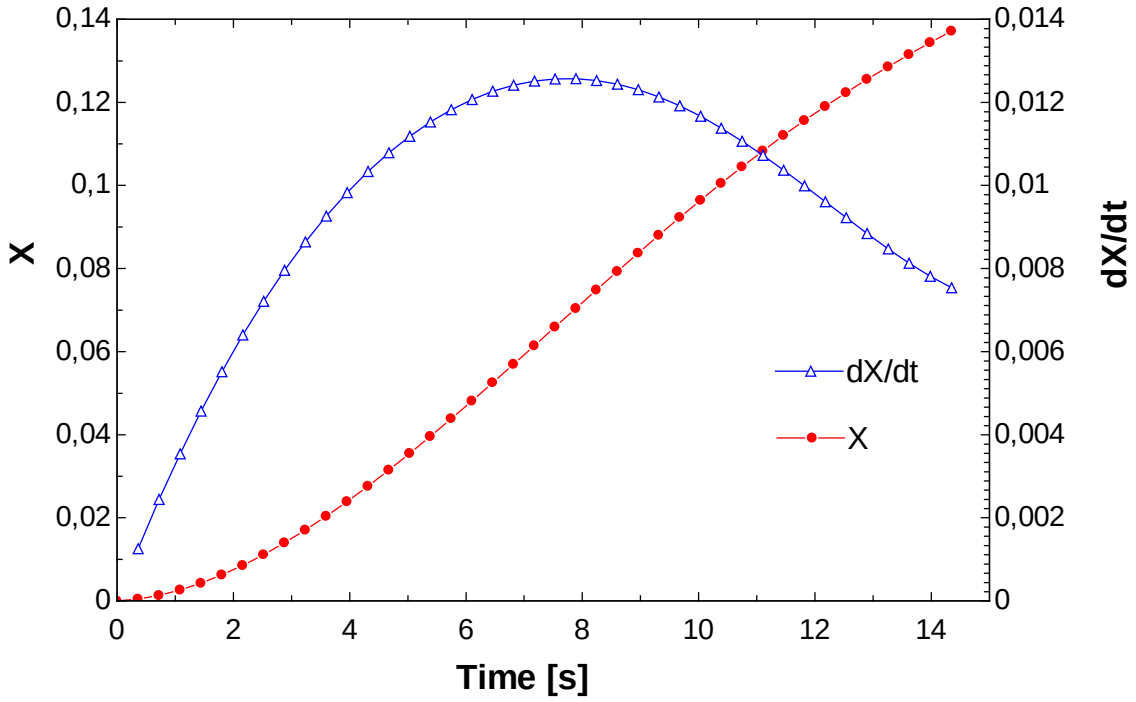

Figure 3-11. Extent of the reaction (red) and its derivative (blue) vs time [s]

The required power to maintain the external wall temperature is large at the bottom of the reactor but compared with "Simulation 1" it has been reduced. The required power lowers until z=0.4 m instead of 1 m where it becomes negative, which means that to maintain the wall temperature constant cooling power is required. In this case, a total heating of 1 kW is required (and 0.5 kW must be subtracted from cooling), which is a 50% less than in the previous simulation (note that in simulation 2 the CO_2 mass flow has been halved).

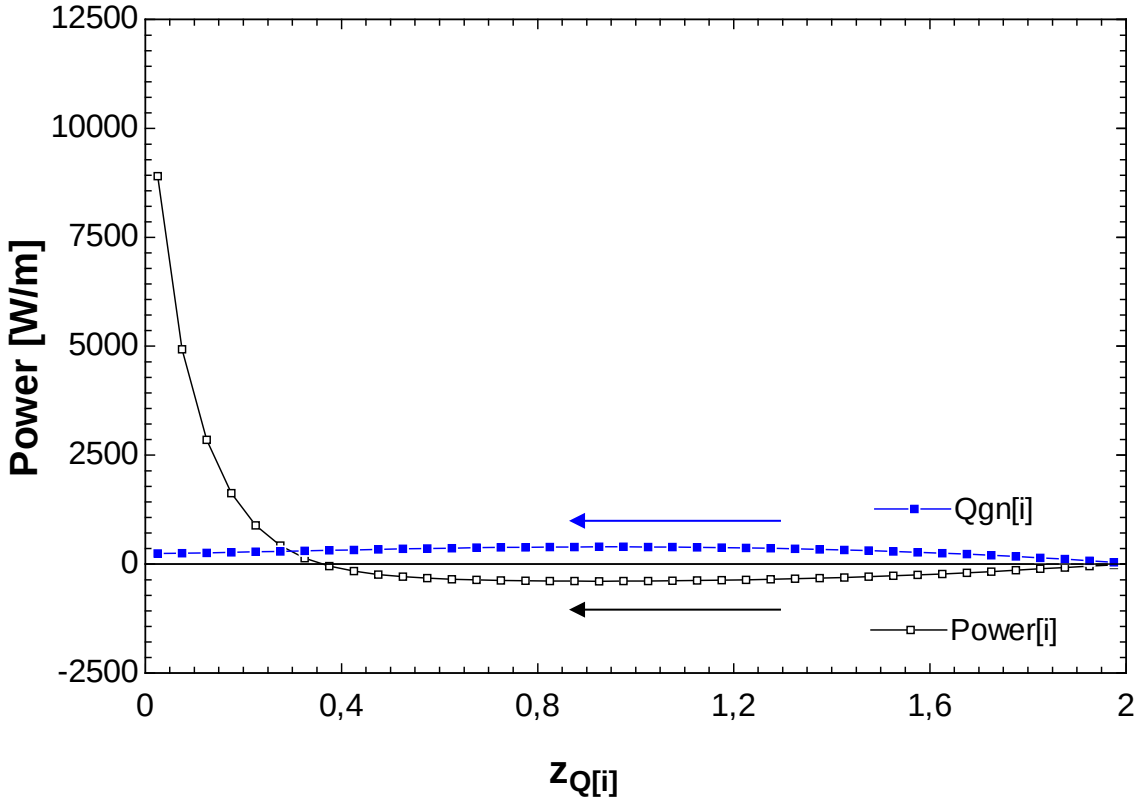

Figure 3-12. Power supplied (black) and power released by the carbonation reaction (blue) to maintain the external wall temperature at 800ºC.

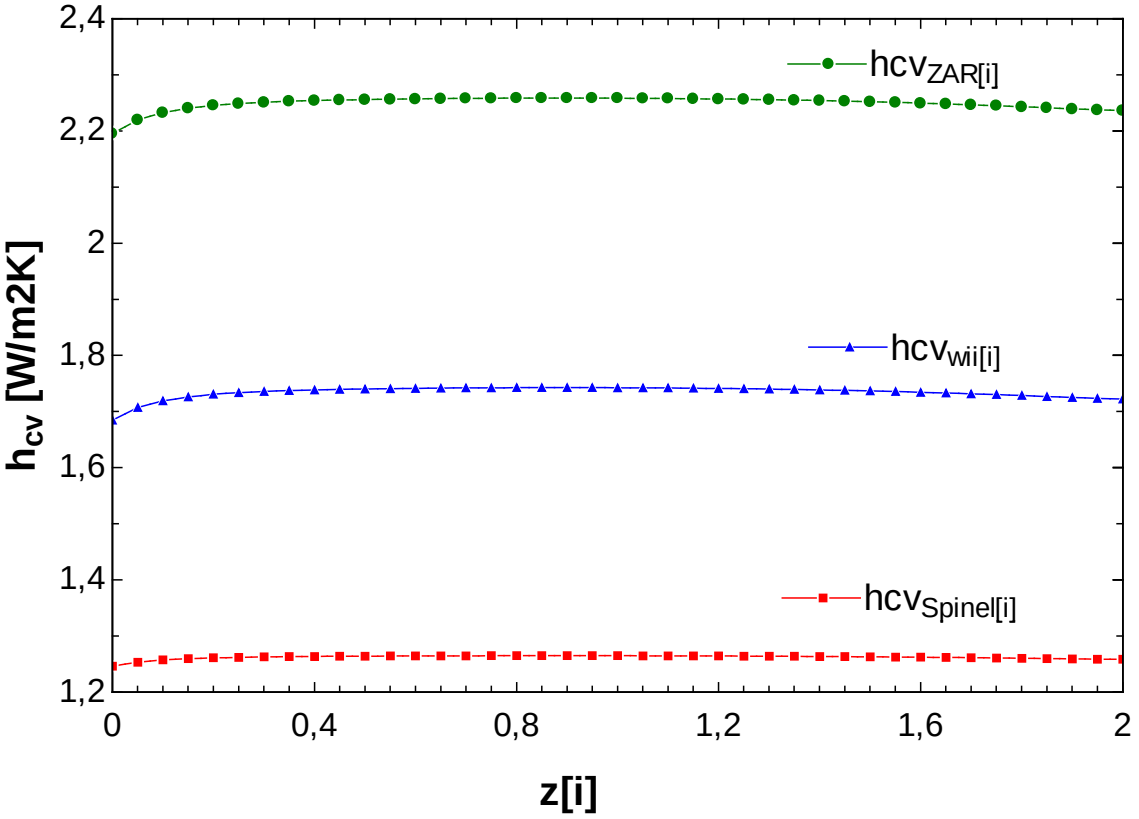

Figure 3-13. Heat transfer coefficients between the gas/particles stream and the carbonator reactor inner wall h (W/m²K) vs Z(m) using 3 different correlations: hcvSpine according to* [3]*, hcvzar according to SOCRATCES deliverable 2.2 and hcvw as calculated in the present model.

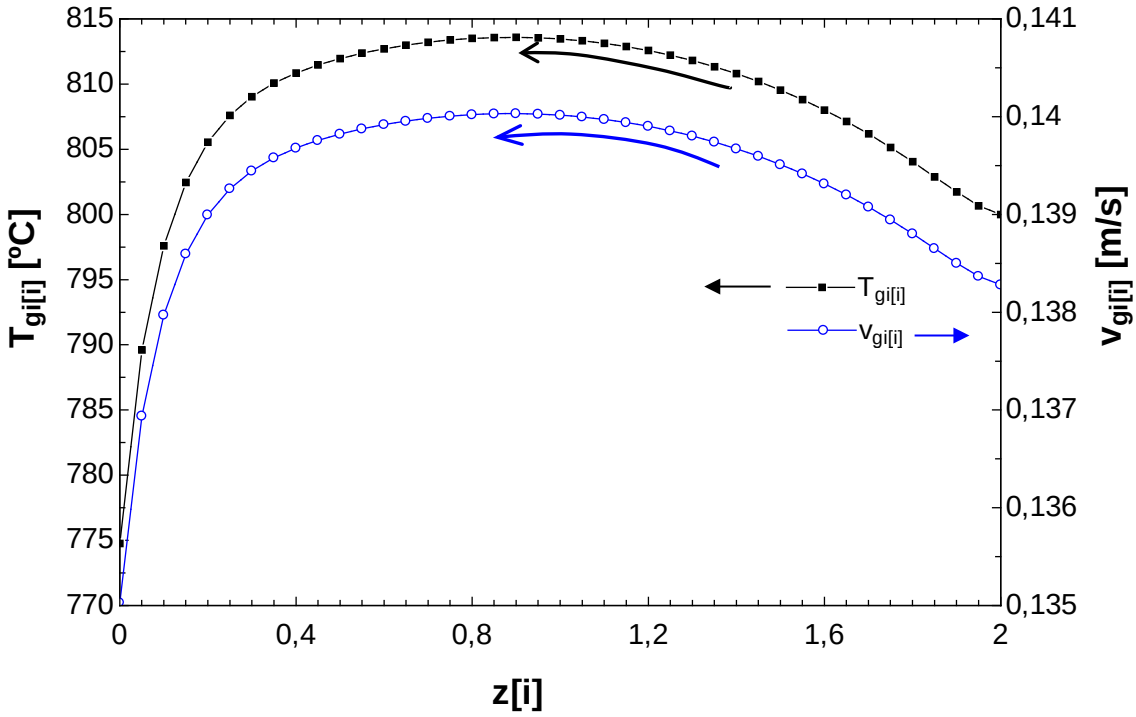

Figure 3-14. Temperature and velocity of the gas-particles stream vs reactor height (m)

Model results according the simulation 2 are summarized in Table 7

Table 8: carbonator results according to simulation 2

Extent of the reaction at the bottom of the carbonator reactor	0.1372
Fraction of the extent of the reaction	68.58%
Average Power supplied (min – max)	266 W/m (-392 W/m to 8.9 kW/m)
Total power supply	1 kW (0.5 kW subtracting cooling power)
Temperature of the exterior wall	800ºC
Residence time	14.35 s

3.3. Simulation 3

In this simulation a faster kinetics is introduced, derived from the experimental results obtained by AUTH within the task 2.1 (Deliverable 2.1). In the same way, a value of CaO conversion at the end of the kinetic-controlled stage of X_k=0.15 is considered. The rest of parameters are the same than in simulation 1 (section 3.1).

In this simulation is shown the behaviour in the second section of the carbonator, which is coupled with the Stirling engine through an HTF (CO_2) taking the carbonator heat. It allows a first approximation to estimate the thermal power provided to the Stirling for a certain inputs values, which in next months will be discussed within the interaction of WP2 and WP4 (power production). As first approach, it is considered that 10 kg/h of CO_2 comes from the Stirling engine at 500ºC.

Table 9. Parameters of Simulation 3.

CARBONATOR			
Type of reactor	Entrained flow reactor	T_{in} CO_2 from storage [ºC]	25ºC
Design temperature	800ºC	T_{out} CO_2=T_{in} carb [ºC]	800ºC
Design pressure	1 bar	T_{in} CO_2 from Stirling [ºC]	500ºC
Design thermal power	10 kWt	ε_{we}= ε_{wei}= ε_{wi}	0.8
Design CaO flow rate	5 kg/h	ε_g	0.12
Design CO_2 flow rate	10 kg/h	ε_{g+p} (calculated)	0.21
Stirling CO_2 flow rate	10 kg/h	ΔL	0.129 m
Reactor length	4 m (2 m+2 m)	h_{spiral} (calculated)	6-15 W/m^2K
Reactor diameter	0.16 m	X_k	0.15
Median particle size, Dv (50)	60µm	a_2	42255 s^{-1}

Figure 3-15 shows the temperature profile along the whole carbonator reactor. In comparison with simulation 1, the faster kinetics make that the almost the entire reaction occurs in the first section of the carbonator, which means that the heat provided for the Stirling under these conditions comes just from the previously heated CO_2 and CaO. This situation must be changed in order to maximize the heat release to the Stirling. Thus, in the application of the tool of the model as support to the design of carbonator, the future analysis will vary the mass flow of all stream (solids, CO_2 from storage, CO_2 recirculation and Stirling CO_2) in order to increase the power production.

Under the conditions of this example, the CO_2 exits the carbonator at more than 600ºC. This hot CO_2 could be recirculated to the carbonator inlet to increase the temperature of the materials entering the carbonator, and therefore enhancing the thermal power released to the Stirling. On the other hand, CO_2 exits the carbonator to the Stirling at 750ºC.

As shown in Figure 3-16, the reaction rate is around 4 times higher that in the simulation 1 because the higher value of pre-exponential factor (a_2) considered.

The higher reaction extent in this simulation regarding simulation 1 allows an important reduction of external power to maintain temperature, to preheat the CO_2 entering the carbonator, as can be seen by comparing Figure 3-18 and Figure 3-5. Since, under these conditions most of the reaction occurs in the first section of the carbonator, heat in excess is released to the preheated CO_2, which causes a higher amount of cooling needs that in simulation

1. This extra cooling means heat losses to the Stirling engine, and therefore it must be avoided by regulating the process streams mass flows or varying the strategy of temperature profiles within the carbonator according to development of reactions.

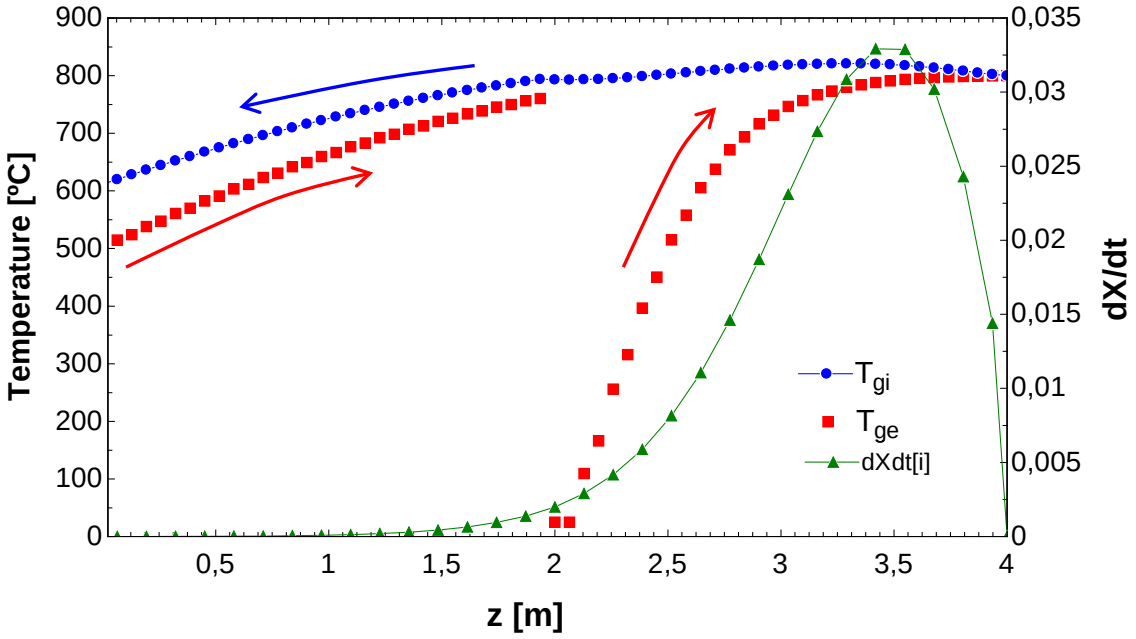

Figure 3-15. Temperature (ºC) profile for the carbonator reactor and the annulus flows (Stirling and pre-heating); and the derivative of the conversion reaction vs reactor height (m).

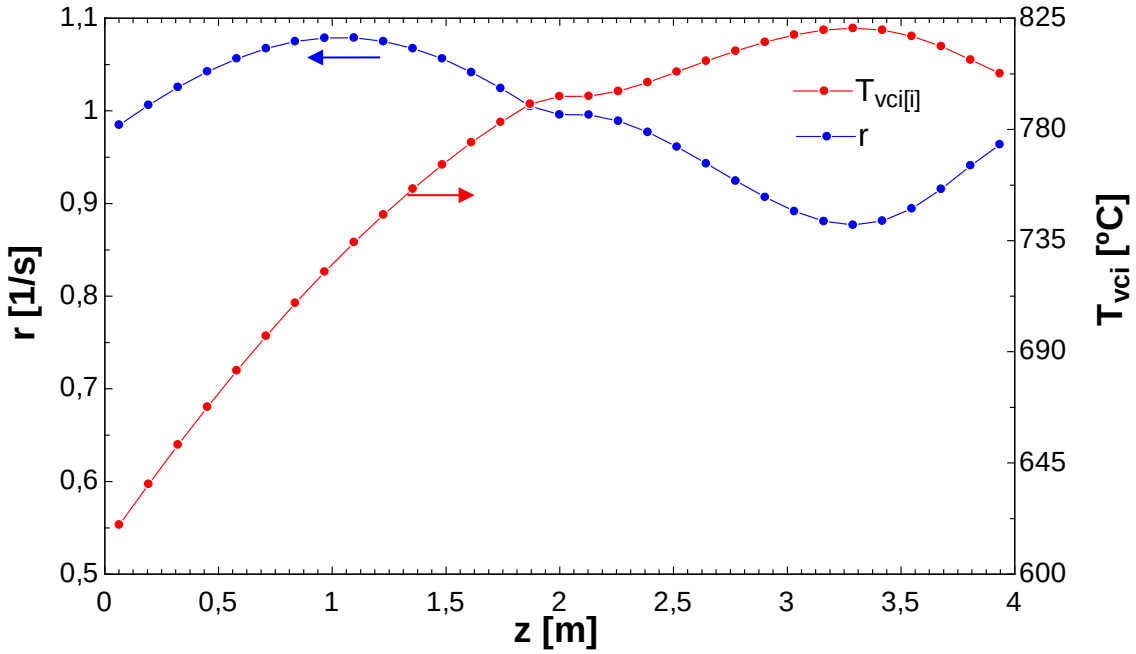

Figure 3-16: Reaction rate (1/s) (blue) and temperature (ºC) vs reactor height (m)

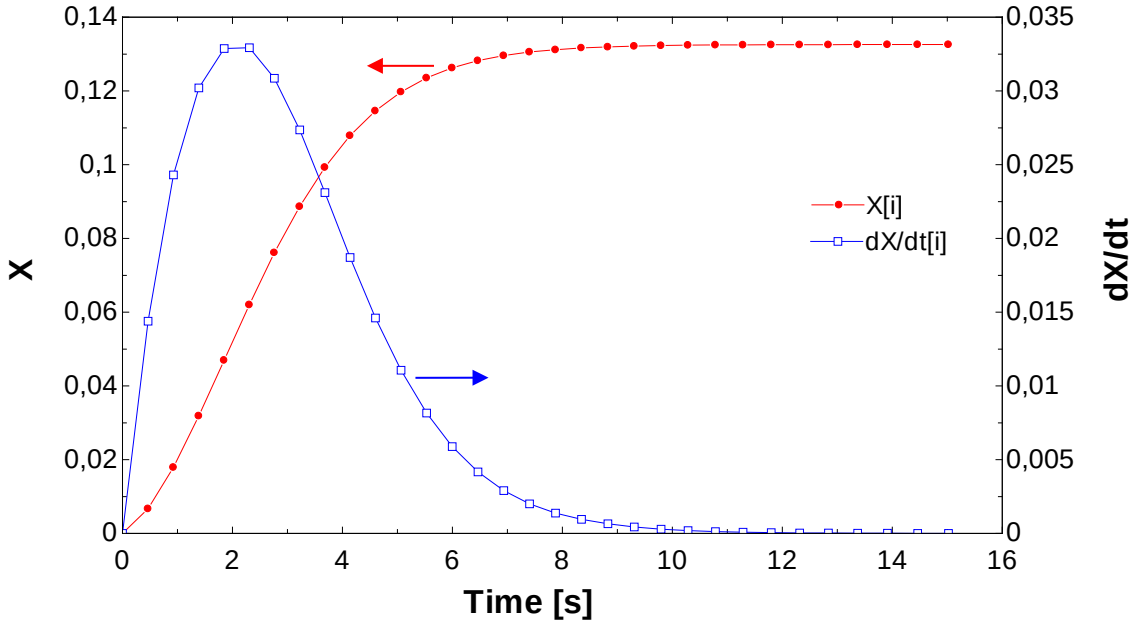

Figure 3-17: Extent of the reaction (red) and its derivative vs time.

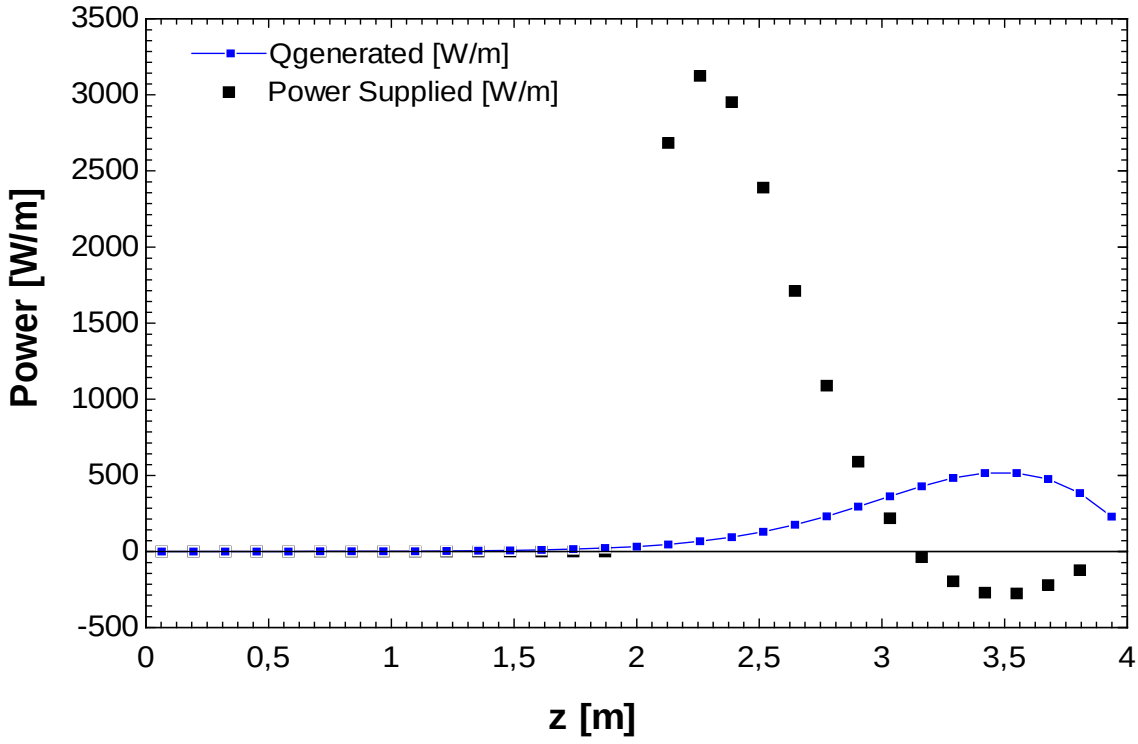

Figure 3-18. Power supplied (black) and power released by the carbonation reaction (blue) to maintain the external wall temperature at 800ºC.

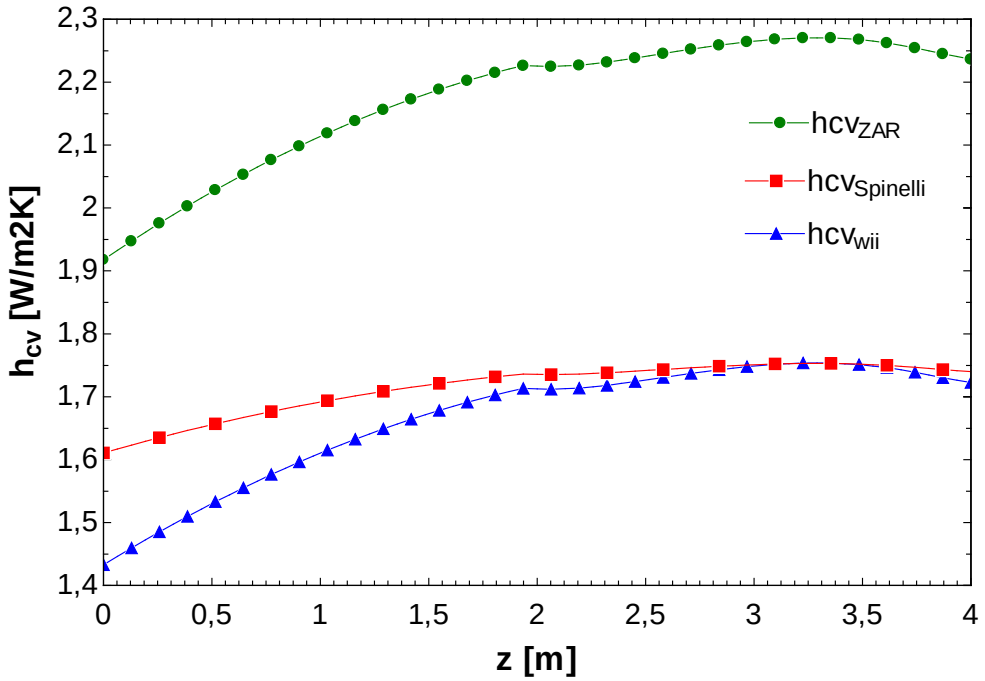

***Figure 3-19. Heat transfer coefficients between the gas/particles stream and the carbonator reactor inner wall h (W/m²K) vs Z(m) using 3 different correlations: $hcv_{Spinelli}$ according to* [3]*, hcv_{ZAR} according to SOCRATCES deliverable 2.2 and hcvw as calculated in the present model based on* [2] .**

Model results according the simulation 1 are summarized in Table 8.

Table 10: carbonator results according to simulation 3

Extent of the reaction at the bottom of the carbonator reactor	0.1326
Fraction of the extent of the reaction	88.38%
Average Power supplied	879 W/m
Total power supply	1.76 kW
Temperature of the exterior wall	800ºC
Residence time	16 s
T out CO_2 to Stirling engine	760ºC

CONCLUSIONS

A novel carbonator model has been proposed within the task 2.3 focused on the analysis of the heat transfer mechanisms within the carbonator reactor. **This model is a tool that will be used to support the carbonator design (WP2) as well as the reactor construction (WP6) within the next months.** Thus, the model is prepared to easily carry out a large number the potential simulations related with this design stage, namely, changes in carbonator operating and design parameters, operation conditions or CaO precursors used in the process. The application of the model on preliminary designs, shows a proper operation of the cooling (CO_2 preheating) system, avoiding temperatures over the equilibrium in the reactor that would freeze, or would invert, the carbonation reaction. Moreover, according to the kinetics results from task 2.1 (deliverable 2.1), the residence time of the particles in the downer reactor seems enough to reach the maximum conversion under the preliminary design conditions. An adequate selection of the CO_2 and CaO mass flow entering the carbonator, the CO_2 recirculation and Stirling engine HFT (CO_2) could guarantee a stable power production power from the carbonation.

These analyses will help to properly estimate the temperature and mass flow of the HTF reaching the power block, which conditions the electric power production, **and therefore optimizing the heat integration between carbonator and power block**. This information can be used within the WP4 (power cycle) to evaluate the power production through the Stirling engine modelling, which subsequent will provide information for both carbonator and power block construction in WP6 (Engineering).

REFERENCES

[1] Y. Ma and J. X. Zhu, “Experimental study of heat transfer in a co-current downflow fluidized bed (downer),” *Chem. Eng. Sci.*, vol. 54, no. 1, pp. 41–50, 1999.

[2] F. P. Incropera and D. P. DeWitt, *Fundamentos de transferencia de calor*. Pearson Educación, 1999.

[3] M. Spinelli, I. Martínez, and M. C. Romano, “One-dimensional model of entrained-flow carbonator for CO2capture in cement kilns by Calcium looping process,” *Chem. Eng. Sci.*, vol. 191, pp. 100–114, 2018.

[4] *VDI Heat Atlas*. Düsseldorf Germany: Springer, 2010.

[5] Y. A. Çengel, *Introduction to Thermodynamics and Heat Transfer*. McGraw-Hill, 2007.

[6] R. Siegel, *Thermal Radiation Heat Transfer, Fourth Edition*. Taylor & Francis, 2001.

[7] F. P. Incropera, D. D. P., T. Bergman, and A. Lavine, *Fundamentals of Heat and Mass Transfer*, 5th ed. New York, 2007.

[8] M. E. Brown, “The Prout-Tompkins rate equation in solid-state kinetics,” *Thermochim. Acta*, vol. 300, no. 1–2, pp. 93–106, 1997.

[9] C. Ortiz, J. M. Valverde, R. Chacartegui, and L. A. Perez-Maqueda, “Carbonation of Limestone Derived CaO for Thermochemical Energy Storage: From Kinetics to Process Integration in Concentrating Solar Plants,” *ACS Sustain. Chem. Eng.*, vol. 6, no. 5, pp. 6404–6417, 2018.

[10] I. Barin, “Thermochemical data of pure substances VCH, Weinheim (1989),” 1989.